

Textures and structures of vapor deposits

D. N. LEE

*Division of Materials Science and Engineering, Seoul National University,
Seoul 151-742, Korea*

The texture of vapor deposits (PVD and CVD) changes from the orientation that places the lowest energy lattice plane parallel to the substrate under the condition of low atom or ion concentration adjacent to the deposit, to the orientation that places the higher energy crystal planes parallel to the substrate as the atom or ion concentration adjacent to the deposit increases. However, in the early stage of deposition, the deposit-substrate interface energy and the surface energy constitute the most important energies of the system. Therefore, if the lattice match is established between the substrate and the deposit without generating much strain energy, the epitaxial growth takes place to reduce the interfacial energy. When the epitaxial growth does not take place, the surface energy is dominant in the early stage of deposition and the lowest energy crystal plane tends to be placed parallel to the substrate up to a critical thickness. The critical thickness depends on the deposition conditions. If the deposition condition does not favor placing the lowest energy crystal plane parallel to the substrate, the initial texture will change to that compatible with the deposition condition as the film thickness increases, and the texture turnover thickness will be short. The microstructure and surface topography of deposits are related to their textures. © 1999 Kluwer Academic Publishers

1. Introduction

Vapour-deposited films are well known to have texture or preferred orientations in them, the texture of the vapour deposits being, in general, dependent on deposition conditions. The present author [1] advanced a model in which a preferred orientation is developed by the selection for survival of grains which are favorably oriented. The model is a growth theory of the development of preferred orientation unlike Walton's nucleation theory [2]. It is generally accepted that a random polycrystalline structure is obtained up to a critical film thickness unless an epitaxial growth condition is satisfied.

The preferred growth model [1] suggests that the texture of physical or chemical vapor deposits changes from the orientation that places the lower surface energy crystal plane normal to the growth direction under the condition of low atom or ion concentration adjacent to the deposit to the orientation that places the higher energy crystal planes normal to the growth direction as the atom or ion concentration adjacent to the deposit increases, unless the deposition temperature is high enough for recrystallization to take place. At such high temperatures, the minimum energy crystal plane tends to be placed normal to the growth direction to minimize the total energy of the system, because the surface energy may be the source of the largest energy in the growing system.

The present author has received many valuable comments. In this paper the model has been elaborated and more experimental results, which are in favor of the model, have been reviewed.

2. Development of preferred orientation

Fig. 1 shows a two-dimensional model of two adjacent crystals. The surface energy of a crystal plane parallel to plane CD of grain A is larger than that of grain B, that is, crystal A has a higher ledge density than crystal B ($\alpha > \beta$). Planes parallel to plane CE must be the most closely packed planes which have the minimum surface energy. Arrows indicate impinging atoms or ions. Squares attached to the surface of the crystal indicate newly condensed atoms.

Atoms are not always condensed directly on to ledges. Atoms condensed on flat surfaces (M in Fig. 1b) are in a less stable state than atoms at ledges, because they are less bonded than atoms at ledges. Therefore, they are liable either to diffuse to ledges or to re-evaporate depending on vapour deposition conditions. The atom concentration adjacent to the deposit will be high at high substrate temperatures and evaporation rates (Fig. 2). This situation may be depicted schematically as shown in Fig. 1b. In this case crystal B is expected to have more atoms condensed between the ledges than crystal A, because the average diffusion distance on crystal A is shorter than on B. Therefore, the configuration on crystal A is more stable than that on crystal B, resulting in the growth of crystal A at the expense of crystal B. In this case the deposit will assume the orientation of crystal A which has a higher surface energy crystal plane normal to the direction of deposit growth. This situation can be equivalent to that for a low polarization in electrodeposition.

The atom concentration adjacent to the deposit will be decreased with decreasing substrate temperature and

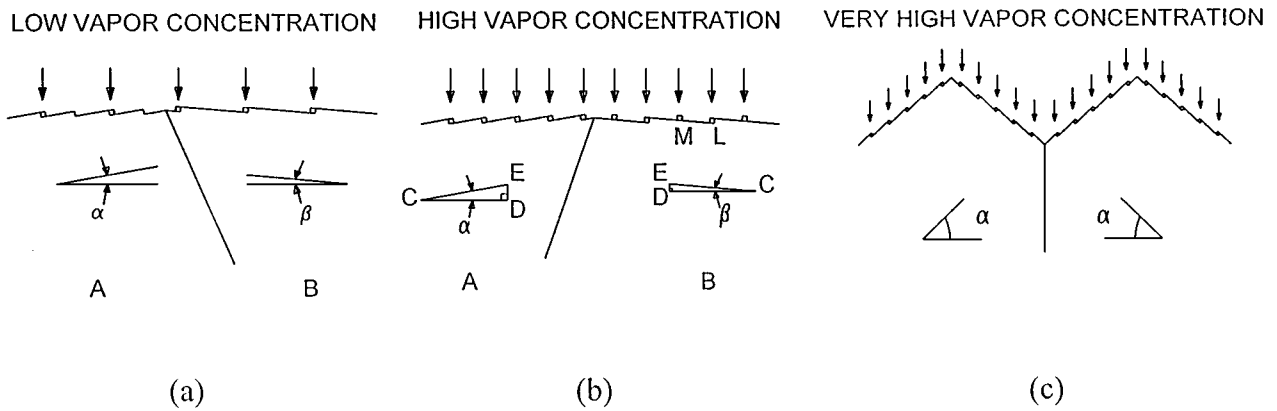


Figure 1 Two-dimensional model explaining development of texture of vapor deposit. Vapor concentration increases in order of (a), (b) and (c).

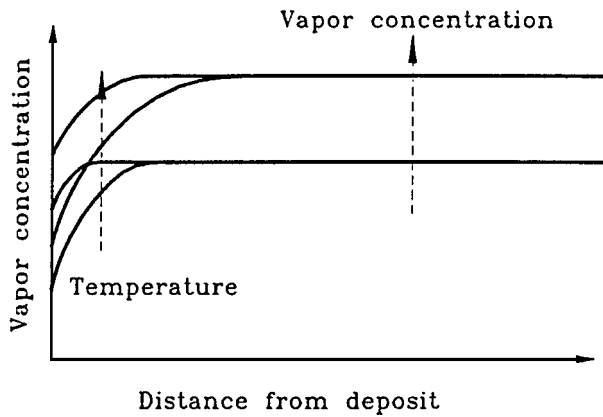


Figure 2 Effects of deposition conditions on depositing material vapor concentration distribution. Arrows indicate increasing directions.

evaporation rate. The situation is shown in Fig. 1a. In this case, the surface area to be covered by condensed atoms is larger for crystal A than for crystal B, because angle α is larger than angle β . Therefore, crystal B will grow at the expense of crystal A. Thus the deposit will assume the orientation of crystal B. It should be noted that the shorter diffusion distance to ledges on crystal A cannot make the crystal grow faster as in the case of high concentration, because atoms are not sufficiently supplied. This situation is similar to the case of a high polarization in electrodeposition.

At sufficiently low temperatures, impinging atoms will be frozen but will not be able to rearrange themselves because low surface diffusion inhibits crystallite

growth and therefore a preferred orientation does not develop. The deposit will consist of very fine grains with a nearly random orientation. On the other hand, when the substrate temperature is high enough to cause recrystallization, the deposit will assume recrystallization textures or nearly random orientations.

This preferred growth model is based on the assumption that the crystal growth front is flat, the direction of impinging ions or atoms is normal to the deposit, the surface diffusion rate is high enough for reduced atoms or condensed species to adjust themselves to stable positions, and the relative lattice surface energies are not influenced by atmosphere.

If the ion or atom concentration is too high for the ledges on flat deposit surface to accept, the deposit surface roughens to increase the ledge density (Fig. 1c). This is compatible with the fact that rough surfaces are often observed in deposits with texture of higher surface energy crystal plane parallel to the substrate plane. If impurity elements like oxygen are codeposited, the crystal growth is hindered by the impurity and the deposit tends to have very fine grains and in turn random orientations.

However, in the early stage of deposition, the deposit-substrate interface strain and free surface energies must be taken into account. If the lattice match is established between the substrate and the deposit, epitaxial growth takes place without generating strain energy to reduce the interfacial energy (Fig. 3a). Epitaxial growth is still possible for a small lattice mismatch (Fig. 3b). However, in this case, the strain energy can be generated

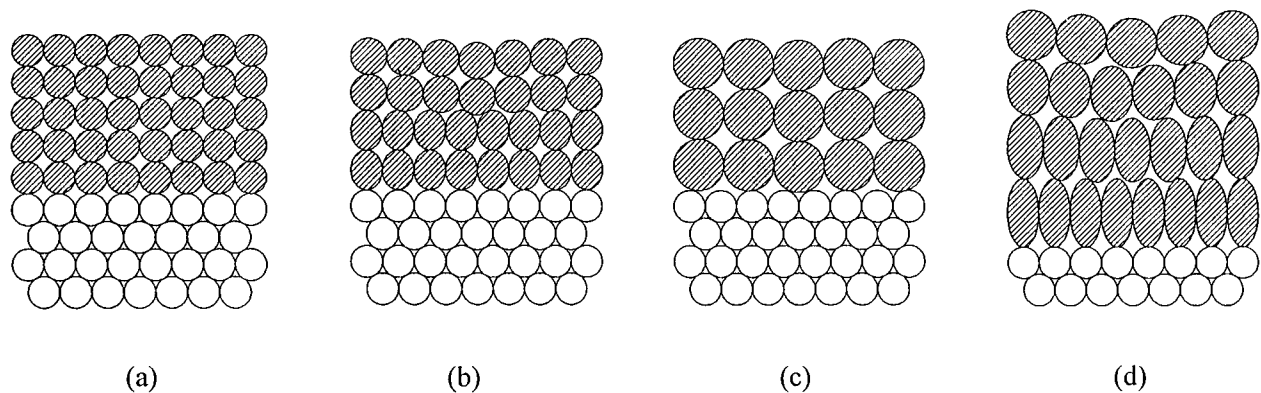


Figure 3 Two-dimensional model explaining (a) epitaxial growth due to lattice match, (b) epitaxial growth due to small lattice mismatch, (c) non-epitaxial growth due to large lattice mismatch and (d) large strain due to epitaxial growth despite of large lattice mismatch.

as shown in strained atoms in Fig. 3b. For a large lattice mismatch between the substrate and the deposit epitaxial growth will not take place (Fig. 3c), because in order for epitaxial growth to take place, very high strain energy can be generated (Fig. 3d). The interface energy for Fig. 3c is higher than for Fig. 3d, in which the strain energy exists. If the interface energy in Fig. 3c is smaller than the interface energy plus the strain energy in Fig. 3d, the situation of Fig. 3c will be more favorable than that of Fig. 3d, resulting in non-epitaxial growth.

The surface layer of the strained deposit is in an equibiaxial plane stress state. If the system is controlled by the strain energy of the surface layer, the lattice plane whose mean biaxial elastic modulus [3, 4] is minimum will be placed parallel to the substrate, whereby the strain energy of the thin deposit becomes minimum. In case of non-epitaxial growth (Fig. 3c), the strain energy will be negligible and new deposit atoms or molecules will try to cover the substrate as closely as possible, whereby the surface energy will be minimized. Once the substrate is covered by a layer of the minimum surface energy lattice plane of deposit, the deposit will grow in the same pattern for the time being, and will not generate grain boundaries. Therefore, the minimum surface energy lattice plane of deposit can be placed parallel to the substrate in the early stage of deposition.

However, this deposit growth will transform into its characteristic growth pattern explained in Fig. 1, as the deposit thickness increases. The turnover thickness of the deposit will depend on the deposition condition. If the deposition condition is far from a condition favoring the minimum surface energy lattice plane being parallel to the substrate, the turnover thickness will be short. When the temperature varies through the thickness, the strain energy of the layer whose temperature is high enough to cause recrystallization may be related to the texture formation. Vapor deposition proceeds by the interaction between vapor and deposit surface. Therefore, the total strain energy of deposit through the whole thickness cannot be related to the texture formation, unless the temperature of the deposit is high enough to cause recrystallization, in which temperature range the atomic mobility in the bulk becomes important. However, it is unlikely that the strain energy will control the texture formation during vapor deposition, unless the situation shown in Fig. 3d takes place.

3. Discussion

3.1. Fcc metals

In fcc metals, the $\{1\ 1\ 1\}$ planes have the smallest surface energy and the $\{1\ 1\ 0\}$ planes have the highest surface energy among low index planes [5]. If other conditions are same, the preferred growth model suggests that the orientation of fcc metals changes from $\langle 1\ 1\ 1 \rangle$ to $\langle 1\ 0\ 0 \rangle$ and finally to near $\langle 1\ 1\ 0 \rangle$ with increasing deposition temperature unless the temperature is high enough to cause recrystallization and low enough to inhibit crystallite growth, because the increase in temperature tends to increase the concentration of vapor atoms or ions adjacent to the growing deposit (Fig. 2). At temperatures high enough for recrystallization to take place, the $\langle 1\ 1\ 1 \rangle$ orientation will be again obtained, because

the surface energy controls the texture of thin films unless the surface energy is modified by surface adsorption. At temperatures low enough to inhibit crystallite growth, the deposit will develop random orientation.

Mah *et al.* [6] studied the preferred orientation of silver coatings which were deposited from a hollow cathode source with substrate bias voltage between 0 and -80 V. Their results were in agreement with the above explanation [1]. Dutta and Wilman [7] studied the texture of silver films deposited at 7×10^{-6} to 7×10^{-3} Torr on glass substrates at room temperature as a function of the film thickness. They observed a random polycrystalline structure up to a critical film thickness. Further deposition led to the successive development of $\langle 1\ 1\ 1 \rangle$, $\langle 1\ 1\ 0 \rangle$, $\langle 1\ 1\ 0 \rangle + \langle 2\ 1\ 1 \rangle$ orientations. They measured the texture using an electron diffraction method. The diffraction patterns did not show well developed spots, which made determination of texture inaccurate. The diffraction pattern indexed as $\langle 1\ 1\ 0 \rangle + \langle 2\ 1\ 1 \rangle$ could be equally well indexed as $\langle 1\ 1\ 0 \rangle + \langle 1\ 1\ 1 \rangle$ by the present author.

Summerizing the results, the texture of silver films indicates the successive development of random, $\langle 1\ 1\ 1 \rangle$, $\langle 1\ 1\ 0 \rangle$, and $\langle 1\ 1\ 1 \rangle$ with increasing film thickness. The texture development can be attributed to an increase in temperature of the deposit due to the heat of condensation of atoms to form a lattice (condensation heat of silver: 2633 J/g at 298 K) and radiant heat from the hotter source of vapor. In the early stage the substrate temperature was so low that the random orientation was obtained. As the temperature increases, the mobility of atoms increases and condensing atoms will try to cover the deposit surface as closely as possible, whereby the surface energy will be minimized, resulting in the $\langle 1\ 1\ 1 \rangle$ orientation. The further increase in surface temperature can give rise to the higher vapor concentration adjacent to the deposit (Fig. 2), which in turn placed the higher surface energy lattice plane $\{1\ 1\ 0\}$ parallel to the substrate forming the $\langle 1\ 1\ 0 \rangle$ orientation. If the temperature increases high enough to cause recrystallization, the recrystallization texture $\langle 1\ 1\ 1 \rangle$ will be developed. The recrystallization texture of most fcc metal films in vacuum is $\langle 1\ 1\ 1 \rangle$.

The texture turnover with increasing film thickness is often attributed to an increase in strain energy of the deposit to the substrate. If the strain energy controlled the texture, the $\langle 1\ 0\ 0 \rangle$ texture would have been obtained, because the mean biaxial elastic modulus of fcc metals is calculated to be minimum in the $\{1\ 0\ 0\}$ planes [3, 4].

Thornton [8] studied the texture of copper and aluminum alloy coatings sputter deposited on glass and stainless steel substrates in the post and hollow cathodes at various argon pressures and temperatures. The results could be explained based on the present model [1]. Rodbell *et al.* [9] studied the texture of sputtered $1\ \mu\text{m}$ thick Al-0.3%Pd films and Al-0.5%Cu films. A strong $\langle 1\ 1\ 1 \rangle$ texture was found in Al-Cu films deposited on 100°C amorphous SiO_2 . A stronger $\langle 1\ 1\ 1 \rangle$ texture resulted when Al-Cu was deposited on 25 nm thick, $\langle 0\ 0\ 0\ 2 \rangle$ textured titanium layer. Al-0.3%Pd films, however, exhibited a weak $\langle 1\ 1\ 1 \rangle$ or $\langle 1\ 1\ 0 \rangle$ texture, which may be approximated by the random orientation,

when deposited on SiO₂ (no heat, 7 cm/s scanning rate), which reverted to a strong (1 1 1) texture when deposited on 25 nm titanium.

The experimental results indicate that the sputtered Al-0.5Cu films were obtained under a condition which makes the minimum surface energy lattice plane placed parallel to the substrate. However, the Al-Pd films obtained under similar conditions had the nearly random orientations possibly due to; (1) palladium has negligible solubility in aluminum, whereas copper has a limited solubility, (2) the Al-Pd films were deposited on the colder substrate than the Al-Cu films, and (3) palladium has the lower condensation heat (3542 J/g at 273 K) than copper (5305 J/g at 273 K). The undissolved palladium may be more effective in blocking rearrangement of condensed atoms especially on the colder substrate; the temperature of which is expected to increase less at the lower condensation heat, which in turn will give rise to the nearly random orientation.

The stronger (1 1 1) texture of Al-0.5Cu films and the strong (1 1 1) texture of Al-0.3Pd when deposited on the (0 0 2) textured titanium layer is attributed to the fact that the closest interatomic distance on the (1 1 1) plane of aluminum crystal (0.2862 nm) differs from the closest interatomic distance on the (0 0 2) plane of titanium (0.29504 nm) only by 3 pct. Thus, the lattice match between close packed planes of Al (1 1 1) and Ti (0 0 2) is almost perfect.

Onoda *et al.* [10] studied effects of the insulator surface roughness on the overlying aluminum alloy film orientation in Al-0.8%Si-0.3%Cu(700 nm)/Ti(50 nm)/Tetra-ethyl-ortho-silicate-O₃ based SiO₂ (800 nm) insulator layered structures. The surface roughness of smooth surface insulators which were prepared by chemical-mechanical-polishing (CMP) was 0.48 nm (Rms), whereas that of rough insulators were 12.2 nm (Rms). On those insulators, the Ti and Al alloy films were sequentially sputter-deposited using a multi-chamber dc-magnetron sputtering system having a base pressure of 2×10^{-8} Torr. The substrate temperatures during deposition were 373 K for Ti film and 0–723 K for Al alloy films.

The titanium films showed a strong (0 0 2) texture on the smooth insulator (The authors reported Ti had preferred orientations of (0 0 2) and (0 1 $\bar{1}$ 1). But, considering $I_{(01\bar{1}1)}/I_{(0002)} = 100/26$ for randomly orientated specimens, the Ti film orientation must be (0 0 2) for almost the same measured X-ray intensities of $I_{(01\bar{1}1)}$ and $I_{(0002)}$.) and equal to the random orientation on the rough insulator. The strong (0 0 2) texture on the smooth insulator is expected from the low substrate temperature (Section 3.3). Even though a film has some orientation with respect to the substrate surface detail, the film on a rough surface substrate will not show a well developed preferred orientation on average, where a nearly random orientation is achieved on the rough insulator.

However, the effect of substrate roughness on the deposit orientation decreases with increasing deposit thickness, and the deposit assumes the texture which is peculiar to the deposition condition, because favorably oriented grains grow at the expense of unfavorably oriented grains. This can be seen from the similar

Al (1 1 1) peak intensities measured for both the CMP and non-CMP samples (Note that the Al alloy film is 700 nm thick, whereas the Ti film is 50 nm thick). The (1 1 1) texture of Al alloy film may be attributed to the high substrate temperatures of 493–723 K, which is thought to be higher than the recrystallization temperature of the film. The intensity of the (1 1 1) orientation of Al alloy film on Ti/smooth insulator is drastically increased by epitaxial relations of Al (1 1 1)//Ti (0 0 2) and Al (1 1 1)//Al₃Ti (1 1 2)//Ti (0 0 2), where Al₃Ti is thought to form by reaction between Al and Ti layers at the substrate temperature of 723 K. On the other hand, the intensity of the (1 1 1) orientation of Al alloy film on Ti/rough insulator is rather drastically decreased by the above epitaxial relations, because the strong (1 1 1) oriented growth normal to the rough asperity surface gives rise to a decrease in the (1 1 1) intensity on average.

3.2. Bcc metals

At low argon pressures and T/T_m , bcc chromium and molybdenum coating sputter deposited on glass and stainless steel substrates in the post and hollow cathodes had the (1 1 0) orientation [12]. The (1 1 0) texture is common for the growth of molybdenum thin films on amorphous substrates by various methods [13] including sputter-deposited multilayers and films [14, 15]. Titanium coatings sputter deposited on liquid nitrogen-cooled glass substrates were in bcc β phase with the (1 1 0) orientation [12].

Drusedau *et al.* [16] studied the texture and surface topography of molybdenum thin films deposited on a silica substrate kept by 470 K by magnetron sputtering. Argon pressure was varied between 0.45 and 4.7 Pa and the deposition rate was less than 0.1 nm/s. The density of the films decreased monotonically with increasing argon pressure from 96% to 48% of bulk Mo. The low density films were amorphous and nanocrystalline with (1 1 0) texture at thicknesses of 30 nm and 3 μ m, respectively. For the dense films (density around 96%) deposited at 0.45 Pa, the 23 nm thick film had only the (1 1 0) peak; a (1 1 2) peak appeared in the 290 nm thick film, and became the dominant signal in the 990 nm thick films. For the 290 nm specimen, a peak related to Mo₅Si₃ appeared, which is thought to be related to interfacial reactions between the silica substrate and the molybdenum film. Upon increasing the film thickness to 2.6 μ m, the peak related to Mo₅Si₃ monotonically decreased and a peak related to MoSi₂ appeared. The surface roughness of the films increased with thickness from 0.8 to 7 nm.

The above results indicate a turnover of the film texture with film thickness from the (1 1 0) texture to the (1 1 2) texture. The turnover of texture can be explained based on the present model. As already mentioned, the most probable initial texture of molybdenum is the (1 1 0) texture. As the thickness increases, the temperature of the film surface increases, because the heat of condensation of the molybdenum vapor (6851 J/g at 500 K) is increasingly difficult to remove as the film thickness increases at a given substrate temperature. The formation of molybdenum silicides reflects the increase in film temperature. The increase in temperature

will increase the concentration of metallic vapor adjacent to the film surface, which in turn will place the higher surface energy lattice plane parallel to the substrate plane. This may lead to the development of the $\langle 1\ 1\ 2 \rangle$ texture in thicker films. The increase in surface roughness with thickness is also expected, as shown in Fig. 1c.

The texture turnover may be argued to be attributed to an increase in strain energy of a deposit as its thickness increases. The difference between the calculated biaxial moduli for the $\langle 1\ 1\ 0 \rangle$ and $\langle 1\ 1\ 2 \rangle$ orientations is negligible (the biaxial moduli of $\langle 1\ 1\ 0 \rangle$ and $\langle 1\ 1\ 2 \rangle$ are calculated to be 447.45 and 444.6 GPa, respectively, at room temperature) and so the strain energy effect can be excluded.

3.3. Hcp metals

Jang [17], in his RF sputtered Co-Cr deposits, found an unusual phenomenon that deposits formed on water cooled polyimide substrates had a larger grain size than deposits formed on 473 K polyimide substrates. Fig. 4 shows TEM images and SAD patterns of 50 nm thick Co-17%Cr films formed on water cooled and 473 K polyimide substrates. The SAD pattern of the film deposited on the water cooled substrate shows very strong $(2\ 0\ \bar{2}\ 0)$, $(1\ 1\ \bar{2}\ 0)$ and $(1\ 0\ \bar{1}\ 0)$ rings suggesting a good c -axis alignment to the growth direction, whereas $(0\ 0\ 0\ 2)$, $(1\ 0\ \bar{1}\ 1)$, $(1\ 0\ \bar{1}\ 2)$ and $(1\ 0\ \bar{1}\ 3)$ rings which should be excluded for a good c -axis alignment appear with relatively strong intensity in the film formed on the 473 K substrate. These results are in agreement with the prediction of the preferred growth model in which a good c -axis alignment to the growth direction is favored at lower deposition temperatures.

Fig. 4 also shows that the film deposited on the water cooled substrate has the larger grain size than the film formed on the 473 K substrate. This is opposite to the usual observation that the lower temperature gives rise to the finer grains. The grain size will depend on the surface and grain boundary energies. If the grain boundary energy is independent of texture, the deposit in which a smaller surface energy plane is placed parallel to the substrate is expected to have larger grains in order to reduce the film energy. Thus, the coarser grains in the deposit formed on the water cooled substrate is thought to be due to the $[0\ 0\ 0\ 2]$ texture. A similar result was observed in fcc copper electrodeposits [18, 19], in which the $\langle 1\ 1\ 1 \rangle$ deposit showed lower strength than a $\langle 1\ 1\ 0 \rangle$ deposit when they were obtained at similar deposition conditions, due to the presence of coarser grains obtained at low temperature [20]. Additional results are given in papers by Jang *et al.* [21, 22]. If the texture is the same, the grain size decreases with decreasing deposition temperature.

3.4. TiN

TiN films are widely used as a coating material due to their high melting point and hardness, good erosion and corrosion resistance, and good conductivity. The film is typically prepared by physical vapor deposition (PVD) or chemical vapor deposition (CVD). The texture of TiN films is known to vary with fabrication conditions.

Je *et al.* [23] studied the texture of TiN films grown on Si $(0\ 0\ 1)$ substrates kept at 375 K by radio frequency (RF) magnetron sputtering in an X-ray sputtering chamber in which a TiN target was placed 10 cm away from the substrate. The sputter gun was operated with RF

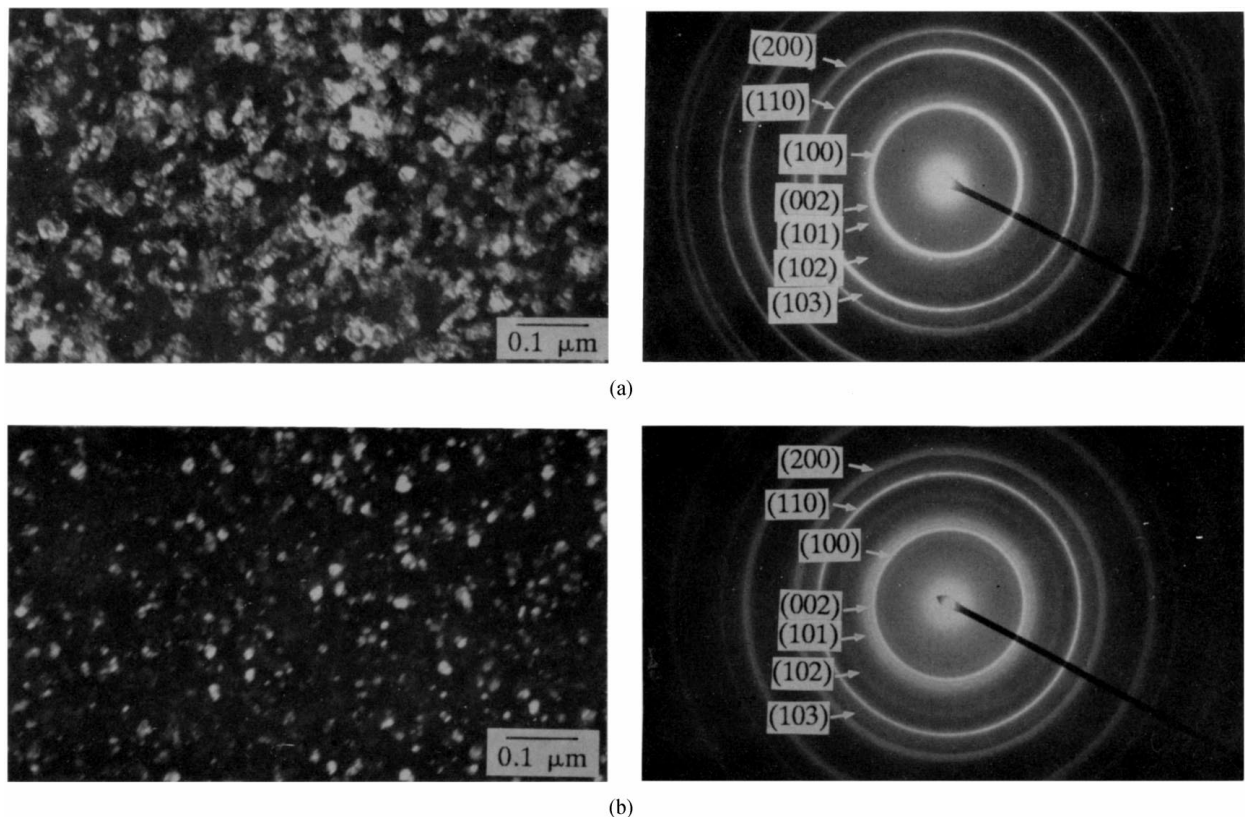


Figure 4 TEM dark field images and SAD patterns of 50 nm thick Co-17%Cr films RF sputtered on (a) water cooled and (b) 473 K polyimide substrates [17].

power between 6 and 12 W/cm². Either 5 × 10⁻³ Torr Ar or a mixture of 5 × 10⁻³ Torr Ar and 1.5 × 10⁻³ Torr N₂ was used as carrier gases.

During the very early stage of the film growth (<23 nm) a random orientation distribution was obtained, indicating that the nucleation and early stage growth took place randomly. Following the random orientation growth, the (002) peak intensity increased rapidly until the film thickness reached about 100 nm. After this stage, the intensity of the (111) peak began to increase rapidly.

In order to explain the result based on the preferred growth model, the relative surface energies of lattice planes of TiN should be known. Unfortunately, even the minimum surface energy plane is not known. Since no measured data are available, there are two different opinions on the minimum surface energy plane. One group thinks that the {111} planes have the minimum energy, while the other group claims that the {100} planes have the minimum energy. The former is based on the fact that TiN can have good conductivity similar to that of metals. On the other hand, Pelleg [24] calculated lattice surface energies based on the fact that TiN has the NaCl structure. According to this calculation, the surface energy increased in order of those of {100}, {110} and {111}. However, TiN has characteristics of metallic, covalent and ionic bonds [25].

The experimental results obtained by Je *et al.* [23] can be explained by the preferred growth model if the {100} planes have the minimum surface energy. The random orientation in the initial stage of the film growth is due to the fact that the substrate temperature (373 K) is too low (m.p. of TiN is 3203 K) for atoms to be adjusted into more stable positions. As the film grows, the temperature of the deposit increases due to heat of condensation, which in turn increases atomic mobility, so that the <100> texture develops, followed by the <111> texture. The turnover from the <100> texture to the <111> texture is compatible with the preferred growth model which places the higher surface energy lattice plane parallel to the substrate at higher temperature. In fact, the deposits with the <111> texture were less strained than those with the <100> texture [23], which reflects the higher temperature in the <111> deposits, resulting in the higher atomic mobility and the less defects.

Je *et al.* [23, 26] attributed the texture turnover to the competition between the surface and strain energies of a film. Their explanation is based on Pelleg *et al.*'s suggestion [24] that the texture in TiN thin films is caused by the lower overall energy of the film which is the sum of the surface and strain energies, and the film would grow toward the {100} planes with the lowest surface energy when the surface energy is dominant, whereas it will grow towards the (111) plane with the lowest strain energy when the strain energy is dominant. Oh and Je [26] attributed the texture turnover from the <100> to <111> to the accumulated strain energy with increasing film thickness. They also claimed that the decrease in the texture turnover thickness with increasing RF sputtering power was due to the increased kinetic energy of the sputtered particles, which was supposed to increase the film strain energy.

However, the film growing process at low temperatures is basically an interaction between the vapor and the deposit surface. Therefore, the total energy of a film cannot be a determining factor in texture formation. If the total energy controls texture, the texture turnover from the <111> to <100> texture will not take place. However, it can happen as will be seen later. The increase in RF power is expected to increase the rate of film temperature rise due to the increased kinetic energy of sputtered particles, which in turn decreases the turnover thickness. Thus the RF power effect on the texture turnover thickness is expected from the preferred growth model.

Je *et al.* [23] also found that the TiN films sputtered at 12 W/cm² with 5 × 10⁻³ Torr Ar underwent the turnover from the <100> to <111> texture with increasing thickness, whereas the films sputtered at 12 W/cm² with a mixture of 5 × 10⁻³ Torr Ar and 1.5 × 10⁻³ Torr N₂ kept the initial texture <100>. The film growth rate also decreased from 1.2 to 0.6 nm/min with the addition of N₂ gas [23]. The result can be explained by the preferred growth model as follows: The decreased growth rate reflects the lower vapor concentration adjacent to the deposit which in turn places the lower surface energy lattice planes {100} parallel to the substrate.

CVD can also yield different textures depending on preparation conditions. Min [27] studied the texture of TiN films prepared on Si (100), Si (111), glass and silica by low temperature CVD in which TiCl₄ and NH₃ were used as the reactive gases and Ar was the carrier gas at a deposition temperature of 973 K. The growth rate of TiN films increased from 0.2 to 30 μm/h with increasing gas flow rate. The growth rate was very much influenced by the NH₃ flow rate. The texture of TiN films changed from the <100> to <110> or <111> orientation with increasing growth rate. However, the films obtained at the initial stage of growth yielded the <100> orientation, regardless of deposition conditions within the experimental range.

The results are in agreement with the prediction of the preferred growth model assuming that the (200) plane has the minimum surface energy as in PVD. The

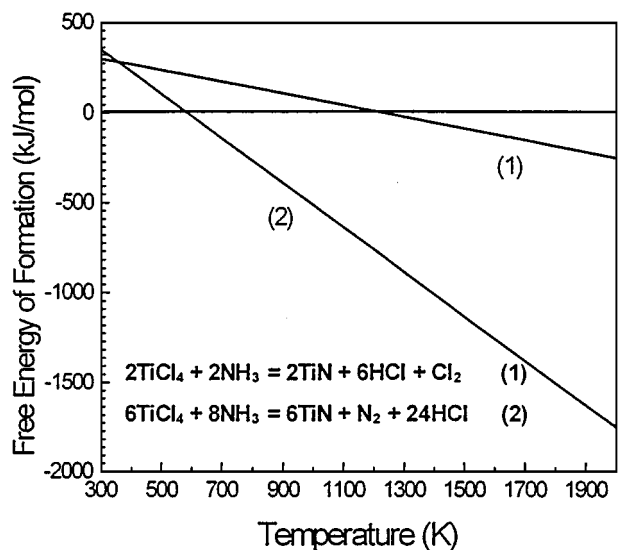
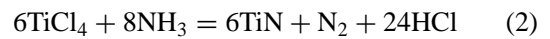


Figure 5 Standard Gibbs free energies of reactions (1) and (2) calculated using data in JANAF Tables [28].

increase in growth rate was achieved by increasing the gas flow rate which increased the vapor concentration adjacent the deposit, and placed the higher surface energy lattice plane parallel to the substrate. Under the deposition conditions which yield the $\langle 100 \rangle$, $\langle 110 \rangle$ and $\langle 111 \rangle$ orientations at 973 K, the decrease in the deposition temperature below 973 K gave rise to the $\langle 100 \rangle$ orientation in agreement with the preferred growth model. As the film thickness increases, grains with the $\langle 100 \rangle$ orientation continued to grow stably under the condition in which the gas concentration adjacent to the growing deposit was low. The $\langle 200 \rangle$ orientation of the film changed to the $\langle 110 \rangle$ or $\langle 111 \rangle$ orientation when the condition favoring the $\langle 110 \rangle$ or $\langle 111 \rangle$ prevailed, and vice versa. If the total strain energy controlled the texture, the inversion from the $\langle 110 \rangle$ or $\langle 111 \rangle$ to the $\langle 100 \rangle$ texture would not have taken place. The pro-

posed following reactions for the formation of TiN are endothermic as shown in Fig. 5.



Therefore, the texture turnover from the $\langle 100 \rangle$ to $\langle 110 \rangle$ or $\langle 111 \rangle$ texture did not take place during film growth unless the deposition condition changed, unlike in PVD.

Jiang *et al.* [29] obtained a similar texture trend in their TiN films prepared by CVD using TiCl_4 , NH_3 and H_2 as reaction gases. They obtained the $\langle 100 \rangle$, $\langle 110 \rangle$ and $\langle 111 \rangle$ textures at graphite substrate temperatures of 1373, 1673 and 1773 K, respectively.

The surface topographies and the cross sectional structures of TiN films are closely related to their

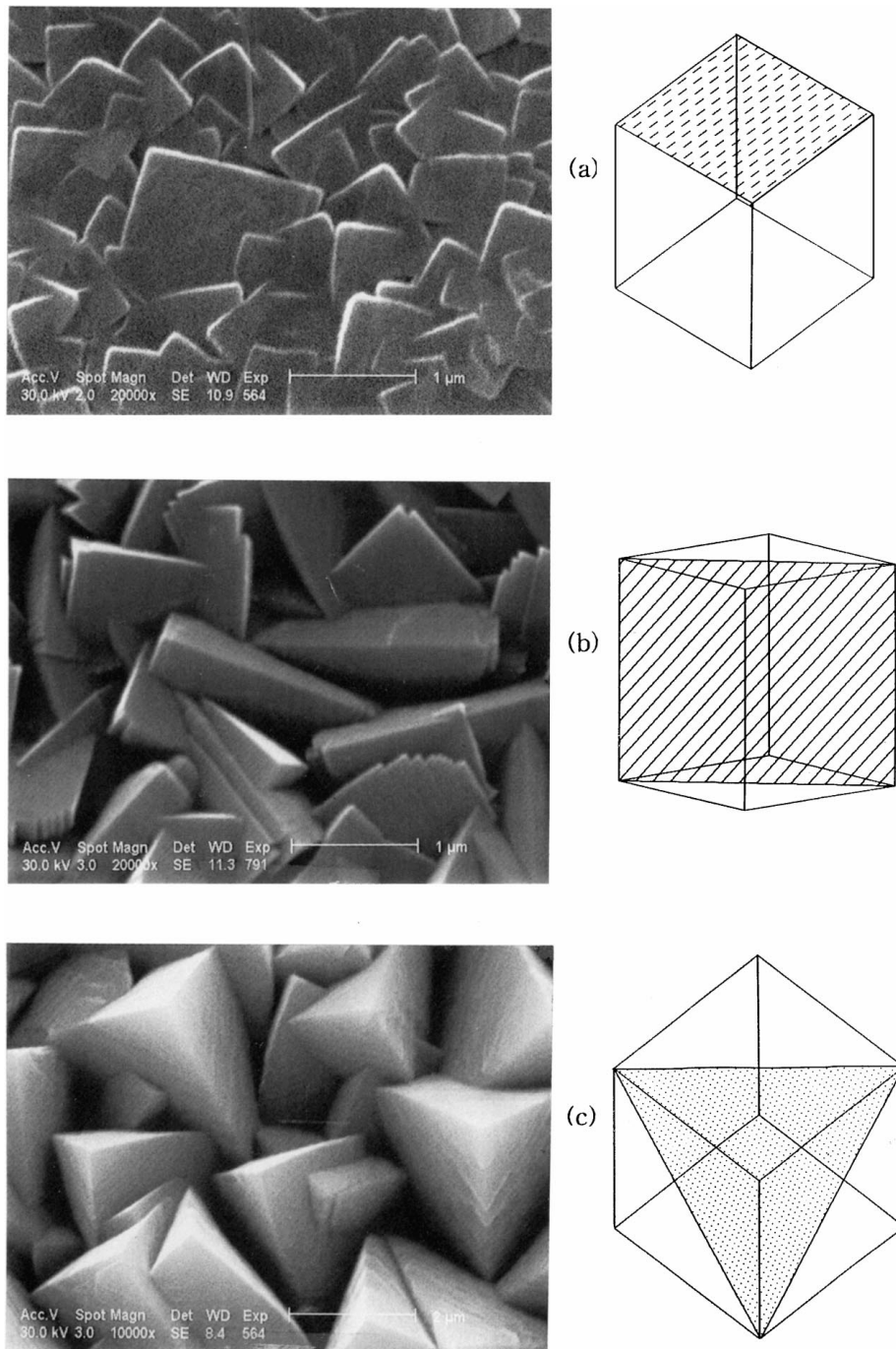


Figure 6 Surface topographies and models of TiN films with (a) $\langle 100 \rangle$, (b) $\langle 110 \rangle$ and (c) $\langle 111 \rangle$ textures [27].

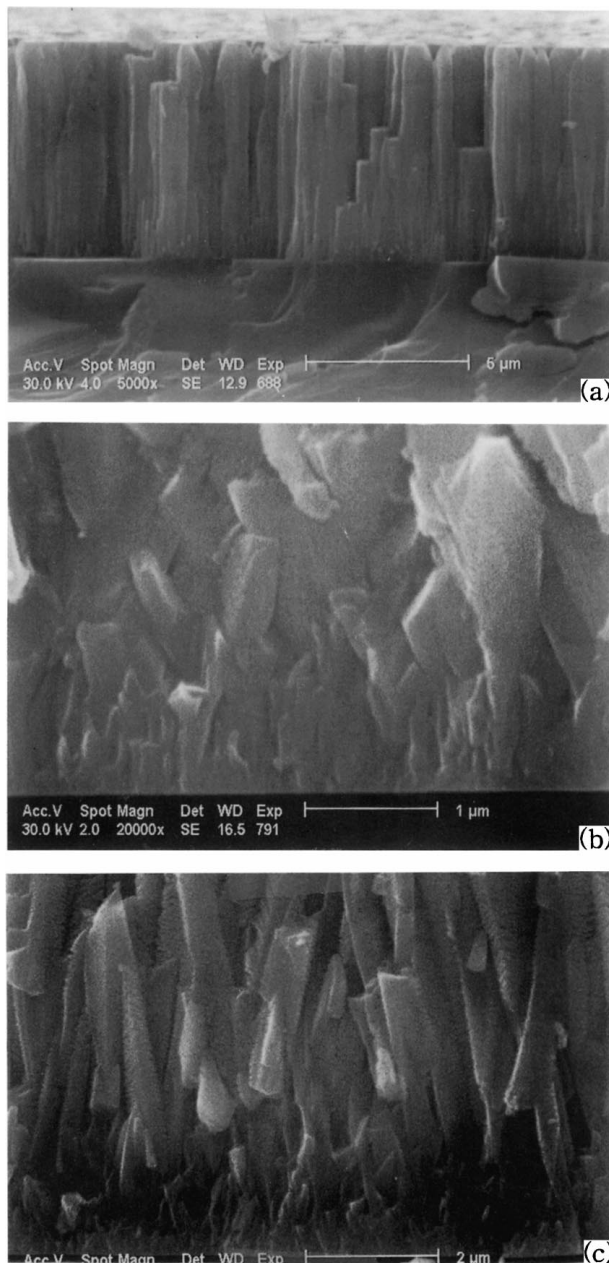


Figure 7 Cross-sectional structures of TiN films with (a) $\{100\}$, (b) $\{110\}$ and (c) $\{111\}$ orientations [27].

textures as shown in Figs 6 and 7, respectively. The surface topographies are easily understood based on the fact that the surfaces are covered with the minimum surface energy lattice planes $\{100\}$. The cross sectional structures indicate that crystals tend to grow along the $\langle 100 \rangle$ directions and normal to the substrate.

4. Conclusion

The texture of vapour deposits changes from the orientation that places the lowest surface energy crystal planes ($\{111\}$ for fcc metals, $\{110\}$ for bcc metals, basal planes for hcp metals, and $\{100\}$ for TiN) parallel to the substrate under the conditions of low atom or ion concentration adjacent to the substrate, to the orientation that places the higher energy crystal planes or the less densely populated atomic planes parallel to the substrate with increasing atom or ion concentration adjacent to the substrate. The bcc metals which have high melting temperatures and low vapour pressure tend to

assume the orientation which place the lowest surface energy crystal facets parallel to the substrate under most evaporating conditions.

The surface topography and the cross-sectional microstructure of vapor deposits are closely related to the their textures.

Acknowledgement

This work has been supported by KOSEF through Research Center for Thin Film Fabrication and Crystal Growing of Advanced Materials, Seoul National University.

References

1. D. N. LEE, *J. Mater. Sci.* **24** (1989) 4375.
2. D. WALTON, *Phil. Mag.* (1962) 1671.
3. J.-H. JEONG, C.-H. CHOI and D. N. LEE, *J. Mater. Sci.* **31** (1996) 5811.
4. W. D. NIX, *Metall. Trans.* **20A** (1989) 2217.
5. B. E. SUNDQUIST, *Acta Metall.* (1964) 1267.
6. G. MAH, P. S. MCLEOD and D. G. WILLIAMS, *J. Vac. Sci. Technol.* **11** (1974) 663.
7. P. K. DUTTA and H. WILMAN, *J. Phys. D: Appl. Phys.* **3** (1970) 389.
8. J. A. THORNTON, *J. Vac. Sci. Technol.* **11** (1974) 663.
9. K. P. RODBELL, D. B. KNORR and J. D. MIS, *J. Electronic Mater.* **22** (1993) 597.
10. H. ONODA, K. TOUCHI and K. HASHIMOTO, *Jpn. J. Appl. Phys.* **34** (1995) L1037.
11. K. KENNEDY, *Trans. Inst. Vac. Met. Soc. AIME* **242** (1968) 2251.
12. K. L. CHOPRA, "Thin Film Phenomena" (McGraw-Hill, New York, 1969) p. 220.
13. L. BERG, G. CZACK, E. KOCH and J. WAGNER, in "Gmelin Handbook of Inorganic Chemistry-Molybdenum Suppl. A 2a," edited by G. Czack, G. Kirscheit, D. Koschel, H. K. Kugler and P. Kuhn (Springer-Verlag, Berlin, 1985) p. 120.
14. J. M. SLAUGHTER, D. W. SCHULZE, C. R. HILLS, A. MIRONE, R. N. WATTS, C. TARRIO, T. B. LUCATORTO, M. KRUMREY, P. MUELLER and C. M. FALCO, *J. Appl. Phys.* **76** (1994) 2144.
15. J. H. SCOFIELD, A. DUDA, D. ALBIN, B. L. BALLARD and P. K. PREDECKI, *Thin Solid Films* **260** (1995) 26.
16. T. DRUSEDU, F. KLABUNDE, M. LOHMANN and J. BLASING, *Phys. Stat. Sol. (a)*, in press.
17. P. W. JANG, Ph.D. thesis, Seoul National University, Seoul, Korea, (1991).
18. D. N. LEE and Y. K. KIM, in Proc. 2nd Asian Metal Finish. Forum, Tokyo, June 1985, p. 130.
19. *Idem.*, *J. Metal Finishing Soc. Korea*, **18** (1985) 95.
20. D. N. LEE, Advanced Metallization for Future ULSI, MRS Symposium Proc., Vol. 427 (1996) p. 168.
21. P. W. JANG, Y. H. KIM, T. D. LEE and T. KANG, *J. Magnetics Soc. of Japan* **13**, Supplement No. S1 (1989) 685.
22. *Idem.*, *IEEE Trans. Magn.* **25** (1989) 4618.
23. J. H. JE, D. Y. NOH, H. K. KIM and K. S. LIANG, *J. Mater. Res.* (1966), rapid communication.
24. J. PELLEGG, L. Z. ZEVEIN and S. LUNGO, *Thin Solid Films* **197** (1991) 117.
25. L. E. TOTH, "Transition Metal Carbides and Nitrides" (Academic Press, New York and London, 1971) p. 248
26. U. C. OH and J. H. JE, *J. Appl. Phys.* **74** (1993) 1692.
27. W. S. MIN, PhD thesis, Seoul National University, Seoul, Korea, (1995).
28. D. STULL and H. PROPHET, "JANAF Thermodynamical Tables," 2nd ed. (National Bureau of Standards, Washington, DC, 1971).
29. C. JIANG, T. GOTO and T. HIRAI, *J. Mater. Sci.* **29** (1994) 669.

Received 15 March

and accepted 23 December 1998